ChemComm

Chemical Communications

Accepted Manuscript

This article can be cited before page numbers have been issued, to do this please use: R. Feng, N. Sato, T. Yasuda, H. Furuta and S. Shimizu, *Chem. Commun.*, 2020, DOI: 10.1039/D0CC00398K.

Volume 54
Number 1
4 January 2018
Pages 1-112

ChemComm
Chemical Communications
rsc.li/chemcomm

ISSN 1359-7345

ROYAL SOCIETY OF CHEMISTRY

COMMUNICATION
S. J. Connon, M. O. Senge *et al.*
Conformational control of nonplanar free base porphyrins: towards bifunctional catalysts of tunable basicity

ROYAL SOCIETY OF CHEMISTRY

rsc.li/chemcomm

View Article Online
DOI: 10.1039/D0CC00398K

COMMUNICATION

Rational design of pyrrolopyrrole-aza-BODIPY-based acceptor-donor-acceptor triads for organic photovoltaics application

Ru Feng,[a] Narumi Sato,[ab] Takuma Yasuda,[ab] Hiroyuki Furuta*[ac] and Soji Shimizu*[ac]

Received 00th January 20xx,
Accepted 00th January 20xx

DOI: 10.1039/x0xx00000x

Acceptor-donor-acceptor triads consisting of diketopyrrolopyrrole (DPP) or pyrrolopyrrole aza-BODIPY (PPAB) or both as acceptors and cyclopentadithiophene as a donor were rationally designed for near infrared (NIR) photovoltaics application. Among them, the PPAB-based triad exhibited the highest power conversion efficiency of 3.88% owing to the panchromatic absorption in the UV/vis/NIR regions.

Diketopyrrolopyrrole (DPP) is a fascinating bicyclic lactam, which has been widely used as an industrial pigment.[1,2] Recently, DPP-based donor-acceptor (D-A) small molecules and polymers have been intensively investigated as functional materials for organic field effect transistors (OFETs)[3–5] and organic photovoltaics (OPVs)[6–10] due to their excellent optical and electronic properties such as efficient charge transport property and high visible absorptivity.[1,2] Owing to the relatively low-lying HOMO levels, the DPP-based materials are promising candidates for OPV application to achieve high open circuit voltage (V_{oc}).[6–10]

Considering the solar irradiance spectrum, panchromatic absorption in the visible and near infrared (vis/NIR) regions is ideal for harvesting solar energy. To achieve such a wide range of light absorption using DPP as a structural basis, various DPP-based π-extended compounds have been intensively investigated in addition to the DPP-based D-A small molecules and polymers.[2,11,12] Recently, we developed a facile method to extend the π-conjugation of DPP using a $TiCl_4$-mediated Schiff base forming reaction[13] to create a dimeric aza-BODIPY analogue, which is referred to as pyrrolopyrrole aza-BODIPY (PPAB).[14] The absorption and fluorescence spectra of a series of PPAB molecules are bathochromically shifted to the NIR region compared with those of the corresponding DPP. As their far-red/NIR absorption and emission is beneficial for bioimaging, sensors and therapeutics, PPABs have been further functionalized toward aggregation-induced emission enhancement (AIEE)[15] and two-photon absorption (TPA)[16] materials and applied to photoacoustic imaging,[17,18] cancer therapy[18] and electrogenerated chemiluminescences (ECLs) in the NIR region.[19] During our study on the aryl-substituent effects on the optical and electrochemical properties of PPABs, we noticed that the dimerization of PPAB by a bithienyl linkage caused significant broadening of the absorption in the vis/NIR region, which is suitable for the far-red/NIR photovoltaics.[20] Considering that a biphenyl-linked PPAB dimer exhibited a single, sharp absorption almost identical to that of the corresponding PPAB monomer due to its twisted structure, the bithienyl linkage played a crucial role in enhancing interchromophore interactions by forming coplanar arrangements of PPAB moieties. Although the panchromatic absorption of the bithienyl-linked PPAB dimer was expected to be ideal for the OPV application, the dimer showed a poor OPV performance with low power conversion efficiency (PCE) of 0.74% and small short circuit current (J_{sc}) of 3.02 mA cm^{-2}.[20] This result implied that suitable bulk heterojunction (BHJ) structures for charge separation were not fabricated due to the low solubility of the dimer.

Taking these results into consideration, we rationally designed a series of triad chromophores (**T1**–**T3**) based on the acceptor-donor-acceptor (A-D-A) structural motif. In these triads, DPP or PPAB or both as acceptors are attached to a cyclopentadithiophene (CPDT) donor bearing branched alkyl chains. The CPDT moiety not only improves the solubility but also enhances the interchromophore interactions. Despite the small molecular size, the absorption spectrum of the PPAB-based triads (**T2** and **T3**) covered a wide range in the UV/vis/NIR regions, which is comparable to those of DPP-based polymers for the NIR photovoltaics.[8–10] The effect caused by replacing

---

[a] *Department of Chemistry and Biochemistry, Graduate School of Engineering, Kyushu University, Fukuoka 819-0395, Japan. E-mail: hfuruta@cstf.kyushu-u.ac.jp, ssoji@cstf.kyushu-u.ac.jp*
[b] *INAMORI Frontier Research Centre (IFRC), Kyushu University, Fukuoka 819-0395, Japan*
[c] *Centre for Molecular Systems (CMS), Kyushu University, Fukuoka 819-0395, Japan*

† Electronic supplementary information (ESI) available: Experimental details, NMR and fluorescence spectra, theoretical calculations and TEM images. See DOI: 10.1039/x0xx00000x

View Article Online
DOI: 10.1039/D0CC00398K

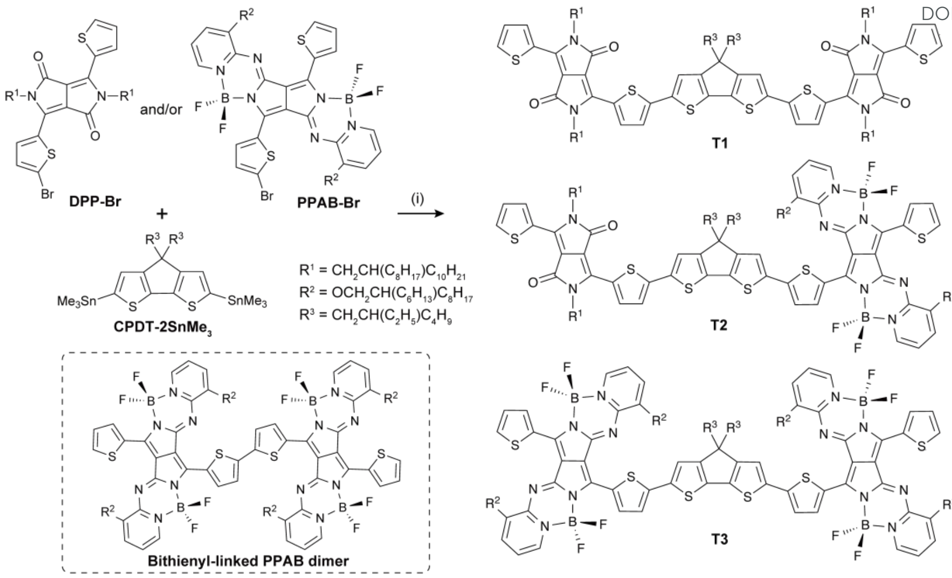

Scheme 1 Synthesis of triads, **T1**–**T3**, and the chemical structure of bithienyl-linked PPAB dimer.[20] Reaction conditions (i): $Pd(PPh_3)_4$ (for **T1**) or $PdCl_2(PPh_3)_2$ (for **T2** and **T3**), toluene, 120 °C.

DPP with PPAB on optical properties and photovoltaic performances were systematically investigated.

The triads (**T1**–**T3**) were synthesized by a Stille coupling reaction[21,22] of bromo-substituted DPP (**DPP-Br**)[23,24] or PPAB (**PPAB-Br**) or both and bis(trimethylstannyl)-CPDT (**CPDT-2SnMe$_3$**).[25] The isolated yields were 38% for **T1** from **DPP-Br**, 48% for **T2** from **DPP-Br** and **PPAB-Br** and 49% for **T3** from **PPAB-Br**. All the compounds were characterized by high-resolution mass spectrometry and ^{1}H NMR spectroscopy (Figs. S1–S6, ESI†).

In chloroform, both **T2** and **T3** exhibited broad absorption in the UV/vis/NIR regions with a maximum at 783 and 827 nm, respectively, whereas the absorption of **T1** was retained in the visible region with a maximum at 648 nm (Fig. 1a). In addition, the molar absorption coefficient (ε) increased from **T1** (0.60×10^4 $M^{-1}cm^{-1}$) to **T2** (1.08×10^5 $M^{-1}cm^{-1}$) and further to **T3** (1.17×10^5 $M^{-1}cm^{-1}$). **T2** also showed another intense band at 626 nm originating from the DPP moiety. Compared with the absorption spectra of the corresponding DPP and PPAB monomer species (Fig. S7, ESI†),[14] the absorption edges shifted to the red due to the effective interchromophore interactions via the CPDT moiety in coplanar conformations. According to our previous study on the bithienyl-linked PPAB dimer,[20] a shoulder band at 709 nm can be ascribed to the contribution of rotational isomers with twisted orientations of the PPAB moieties, which exhibit monomer-like absorption due to minor interchromophore interactions. In the drop-cast film state, the triads exhibited slight broadening and red-shift of the main absorption bands, denoting the formation of the π-stacked aggregates (Fig. 1b). Despite the small molecular size, the absorbance onset of **T3** in the NIR region is almost comparable to that of DPP-based polymers used for NIR photovoltaics.

Although the fluorescence of triads was nearly quenched in solution (ϕ_F = ~0.03) and quenched in the solid state, their fluorescence spectra in solution were diagnostic of the structures. **T1** exhibited a single emission at 724 nm, which was a mirror-image to the absorption spectrum (Fig. S8, ESI†).

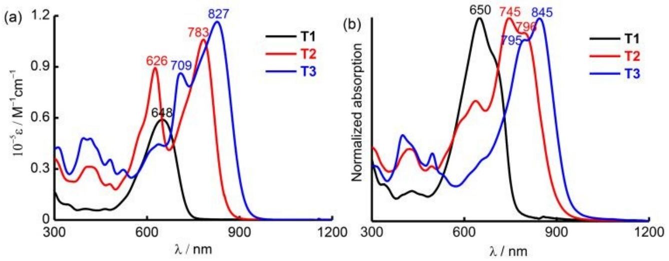

Fig. 1 UV/vis/NIR absorption spectra of **T1** (black), **T2** (red) and **T3** (blue) (a) in chloroform and (b) in a film state.

Similarly, **T2** also showed a single emission originating from the PPAB moiety at 838 nm regardless of excitation wavelengths probably due to the fluorescence resonance energy transfer (FRET) from the DPP moiety to the PPAB moiety. In contrast to these single emissions, **T3** exhibited bimodal emissions at 706 and 898 nm, which is similar to that of the bithienyl-linked PPAB dimer.[20] Although there is continuous distribution of rotational isomers, this can be explained in terms of the coplanar and twisted orientations of the PPAB moieties at the excited state, which may exhibit a mirror-imaged emission at 898 nm to the farthest absorption band at 828 nm and a monomer-like emission at 706 nm, respectively. Considering that such bimodal emission behaviour was not observed for the other triads, a rotational barrier of **T3** from the twisted conformation to the coplanar conformation in the excited should be high so that the conformational change may compete the radiative decay process. Similar bimodal emission behaviours caused by the two extreme conformers have been investigated in detail in the case of porphyrin and corrole dimers.[26,27]

To estimate the redox properties, cyclic voltammetry measurements were performed in dichloromethane containing 0.1 M tetra-*n*- hexafluorophosphate ($nBu_4N{\cdot}PF_6$) as a supporting

View Article Online
DOI: 10.1039/D0CC00398K

Table 1 Summary of optical and electrochemical properties of **T1–T3**

						Solution		Film
Compd.	$E^{1/2}{}_{ox}{}^{a}$ [V]	$E^{1/2}{}_{red}{}^{a}$ [V]	$E_{HOMO}{}^{b}$ [eV]	$E_{LUMO}{}^{c}$ [eV]	$E_g{}^{d}$ [eV]	λ_{max} [nm]	$10^{-5}\ \varepsilon$ [M^{-1} cm^{-1}]	λ_{max} [nm]
T1	0.21	–1.64	–4.96	–3.24	1.72	648	0.60	650
T2	0.22	–1.18	–4.95	–3.70	1.25	626, 783	1.08	745, 796
T3	0.10	–1.19	–4.89	–3.68	1.21	709, 827	1.17	795, 845

[a] Determined by cyclic voltammetry (conditions: 0.5 mM CH_2Cl_2 solutions containing 0.1 M $n$$Bu_4N{\cdot}PF_6$ as a supporting electrolyte at a scan rate of 100 mV s^{-1}). Potentials are given relative to ferrocenium/ferrocene (Fc^+/Fc) couple. [b] $E_{HOMO} = -(E^{ox}_{onset} + 4.8)$ [eV]. [c] $E_{LUMO} = -(E^{red}_{onset} + 4.8)$ [eV]. [d] $E_g = E_{LUMO} - E_{HOMO}$ [eV].

electrolyte (Fig. 2). The triads exhibited simple reduction waves and multiple oxidation waves. Compared with the reduction potentials of the corresponding DPP and PPAB monomers, the reduction observed for **T1** and **T3** (**T1**: –1.64 and –2.27 V vs. Fc^+/Fc, **T3**: –1.19 and –1.74 V) can be assigned as DPP- and PPAB-centred reductions. By referring to the data of these homo-type triads, the first and third reductions of **T2** at –1.18 and –1.79 V and the second and fourth ones at –1.65 and –2.33 V can be ascribed to the PPAB- and DPP-centred reductions, respectively. The multiple oxidations of the triads mainly originate from the CPDT moiety as only one or two oxidation waves were observed for the PPAB dimers in the previous study.[20]

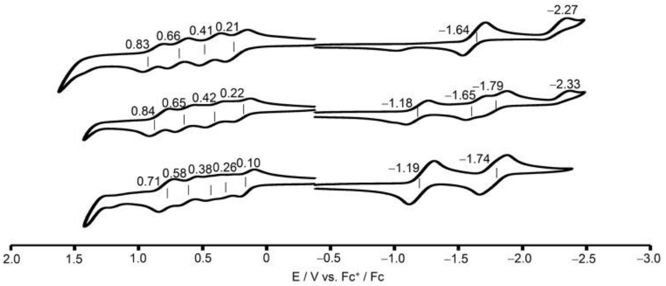

Fig. 2 Cyclic voltammograms of the triads in CH_2Cl_2 (0.5 mM) containing 0.1 M $n$$Bu_4N{\cdot}PF_6$ as a supporting electrolyte at a scan rate of 100 mV s^{-1}.

The HOMO and LUMO energy levels of **T1**–**T3** were estimated based on the first oxidation and reduction potentials of the triads (Table 1), and the DFT and TDDFT calculations at the B3LYP/6-31G(d) level reproduced the trend of their energies and transitions (Tables S1 and S2, Figs. S9–S12, ESI†). As model structures of **T3** for DFT calculations, coplanar and perpendicular extreme conformations were used because the continuous distribution of rotational isomers at the ground state was inferred from the absorption spectra. The LUMO resides shallower (–3.24 to –3.70 eV) than that of [6,6]-phenyl-C_{71} butyric acid methyl ester ($PC_{71}BM$) at –4.3 eV,[28] implying that **T1**–**T3** can be used as p-type materials in OPV devices. The LUMO energy offset between **T1**–**T3** and $PC_{71}BM$ can also facilitate efficient charge separation.[29] The LUMO energy levels of **T2** and **T3** became deeper than that of **T1** due to the stronger acceptor nature of the PPAB moiety than the DPP moiety. The low-lying HOMO energy levels of these triads would also be beneficial to attain large V_{oc} because V_{oc} is directly proportional to the energy gap between the HOMO and LUMO energy levels of the donor and acceptor, respectively.[30,31]

To investigate the photovoltaic properties of the triads as a p-type material, we fabricated solution-processed BHJ-OPVs with an inverted device structure of indium tin oxide (ITO)/ZnO (30 nm)/**T1**–**T3**:$PC_{71}BM$ (70–110 nm)/MoO_x (10 nm)/Ag (100 nm) (Fig. S13, ESI†). The BHJ active layer consisting of **T1**–**T3**:$PC_{71}BM$ binary blend was prepared by spin-coating from their chloroform solutions with or without solvent additives. After optimization of the device fabrication conditions (donor-acceptor (D/A) ratio, thickness of the active layer and additives (Figs. S14–S19 and Tables S3–S8, ESI†)), the **T3**:$PC_{71}BM$ BHJ-OPVs device fabricated in the presence of 1,8-diiodooctane (DIO) as an additive showed the best PCE of 3.88% among the three triads (Fig. 3, Table 2). The PCE values of other triads under the same conditions were 0.18% for **T1** and 1.49% for **T2**. It is noticeable that **T3** exhibited J_{sc} up to 11.7 mA cm^{-2}, which is a reason for its high device performance. This could be attributed to its panchromatic absorption and high absorptivity compared with those of **T1** and **T2**.

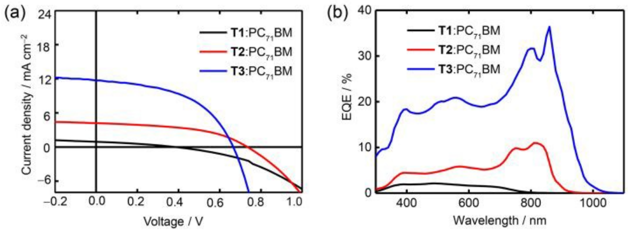

Fig. 3 (a) *J-V* curves and (b) EQE spectra of **T1**–**T3**:$PC_{71}BM$ BHJ-OPVs.

Table 2 Device characteristics of **T1**–**T3**:$PC_{71}BM$ BHJ-OPVs

Blend ratio [a]	Solvent [b]	J_{sc} (mA cm^{-2})	V_{oc} (V)	FF	PCE (%)
T1:$PC_{71}BM$	CF:DIO	0.98	0.43	0.36	0.18
T2:$PC_{71}BM$	CF:DIO	4.20	0.73	0.48	1.49
T3:$PC_{71}BM$	CF:DIO	11.7	0.67	0.50	3.88

[a] Donor-acceptor ratio is 1:2 (w/w), and thickness of the bulk heterojunction layer is 90 nm. [b] CF: chloroform, DIO: 1,8-diiodooctane and the ratio: 99.5:0.5 vol%.

The interior morphologies of the BHJ active layers were characterized by transmission electron microscopy (TEM) (Fig. S20, ESI†). The TEM images of the **T3**:$PC_{71}BM$ blend films revealed homogenous and fine nanostructures with closely mixed D/A networks. The small average domain size of 11 nm scaled based on the D/A segregation for **T3**:$PC_{71}BM$ is favourable for efficient charge separation, which is consistent with its high J_{sc} value. It is, therefore, worth emphasizing that

PPAB-based small molecules are highly promising as new materials in photovoltaic applications.

In this study, we presented three panchromatic A-D-A small molecules, using DPP or PPAB or both as acceptors and CPDT as a donor. We found that the CPDT moiety bearing branched alkyl chains is a suitable mediator to enhance interchromophore interactions. The absorption spectra of **T1**–**T3** indicated that the replacement of DPP with PPAB from **T1** to **T3** broadened the absorption in the UV/vis/NIR region and increased the molar absorption coefficients. In the OPV studies, **T3** exhibited the highest PCE and J_{sc} among the triads due to its panchromatic absorption in the UV/vis/NIR regions and high absorptivity. Our current results demonstrate that the A-D-A structural motif based on PPAB is an effective approach to achieve panchromatic photovoltaics with high PCE values, which can further be improved by optimizing the donor unit. Research along this direction is being intensively investigated in our laboratory.

This work was supported by Grants-in-Aids from JSPS (Nos. JP26708003 and JP19H02703). The authors thank Ms. Natsuko Ide for the TEM measurements.

Conflicts of interest

There are no conflicts to declare.

Notes and references

1 (*a*) J. S. Zambounis, Z. Hao and A. Iqbal, *Nature*, 1997, **388**, 131; (*b*) A. Iqbal, M. Jost, R. Kirchmayr, J. Pfenninger, A. Rochat and O. Wallquist, *Bull. Soc. Chim. Belg.*, 1988, **97**, 615; (*c*) Z. M. Hao and A. Iqbal, *Chem. Soc. Rev.*, 1997, **26**, 203.
2 M. Grzybowski and D. T. Gryko, *Adv. Opt. Mater.*, 2015, **3**, 280.
3 C. B. Nielsen, M. Turbiez and I. McCulloch, *Adv. Mater.*, 2013, **25**, 1859.
4 B. Lim, H. Sun, J. Lee and Y. Y. Noh, *Sci. Rep.*, 2017, **7**, 164.
5 Y. Qiao, Y. Guo, C. Yu, F. Zhang, W. Xu, Y. Liu and D. Zhu, *J. Am. Chem. Soc.,* 2012, **134**, 4084.
6 A. Tang, C. Zhan, J. Yao and E. Zhou, *Adv. Mater.,* 2017, **29**, 1600013.
7 (*a*) W. Shin, T. Yasuda, Y. Hidaka, G. Watanabe, R. Arai, K. Nasu, T. Yamaguchi, W. Murakami, K. Makita and C. Adachi, *Adv. Energy Mater.*, 2014, **4**, 1400879; (*b*) W. Shin, T. Yasuda, G. Watanabe, Y. S. Yang and C. Adachi, *Chem. Mater.*, 2013, **25**, 2549.
8 (*a*) W. Li, K. H. Hendriks, M. M. Wienk and R. A. J. Janssen, *Acc. Chem. Res.,* 2016, **49**, 78; (*b*) M. Li, A. H. Balawi, P. J. Leenaers, L. Ning, G. H. L. Heintges, T. Marszalek, W. Pisula, M. M. Wienk, S. C. J. Meskers, Y. Yi, F. Laquai and R. A. J. Janssen, *Nat. Commun.,* 2019, **10**, 2867; (*c*) G. H. L. Heintges and R. A. J. Janssen, *RSC Adv.,* 2019, **9**, 15703; (*d*) K. H. Hendriks, W. Li, M. M. Wienk and R. A. J. Janssen, *J. Am. Chem. Soc.,* 2014, **136**, 12130; (*e*) W. Li, A. Furlan, K. H. Hendriks, M. M. Wienk and R. A. J. Janssen, *J. Am. Chem. Soc.*, 2013, **135**, 5529.
9 S. Qu and H. Tian, *Chem. Commum.,* 2012, **48**, 3039.
10 G. Oklem, X. Song, L. Toppare, D. Baran and G. Gunbas, *J. Mater. Chem. C*, 2018, **6**, 2957.
11 (*a*) M. Krzeszewski, E. M. Espinoza, C. Červinka, J. B. Derr, J. A. Clark, D. Borchardt, G. J. O. Beran, D. T. Gryko and V. I. Vullev, *Angew. Chem., Int. Ed.*, 2018, **57**, 12365; (*b*) A. Purc, E. M. Espinoza, R. Nazir, J. J. Romero, K. Skonieczny, A. Jeżewski, J. M. Larsen, D. T. Gryko and V. I. Vullev, *J. Am. Chem. Soc.*, 2016, **138**, 12826; (*c*) M. Grzybowski, A. Jeżewski, I. Deperasińska, D. H. Friese, M. Banasiewicz, V. Hugues, B. Kozankiewicz, M. Blanchard-Desce and D. T. Gryko, *Org. Biomol. Chem.,* 2016, **14**, 2025; (*d*) D. H. Friese, A. Mikhaylov, M. Krzeszewski, Y. M. Poronik, A. Rebane, K. Ruud and D. T. Gryko, *Chem. – Eur. J.,* 2016, **21**, 18364; (*e*) M. Grzybowski, V. Hugues, M. Blanchard-Desce and D. T. Gryko, *Chem. – Eur. J.*, 2014, **20**, 12493; (*f*) S. Richert, S. Mosquera Vazquez, M. Grzybowski, D. T. Gryko, A. Kyrychenko and E. Vauthey, *J. Phys. Chem. B*, 2014, **118**, 9952.
12 (*a*) G. M. Fischer, E. Daltrozzo and A. Zumbusch, *Angew. Chem., Int. Ed.*, 2011, **50**, 1406; (*b*) W. J. Akers, C. Kim, M. Berezin, K. Guo, R. Fuhrhop, G. M. Lanza, G. M. Fischer, E. Daltrozzo, A. Zumbusch, X. Cai, L. V. Wang and S. Achilefu, *ACS Nano*, 2011, **5**, 173; (*c*) G. M. Fischer, C. Jüngst, M. Isomäki-Krondahl, D. Gauss, H. M. Möller, E. Daltrozzo and A. Zumbusch, *Chem. Commun.*, 2010, **46**, 5289; (*d*) G. M. Fischer, M. Isomäki- Krondahl, I. Göttker-Schnetmann, E. Daltrozzo and A. Zumbusch, *Chem. – Eur. J.*, 2009, **15**, 4857; (*e*) M. Fischer, A. P. Ehlers, A. Zumbusch and E. Daltrozzo, *Angew. Chem., Int. Ed.*, 2007, **46**, 3750.
13 (a) S. Shimizu, A. Murayama, T. Haruyama, T. Iino, S. Mori, H. Furuta and N. Kobayashi, *Chem. – Eur. J.*, 2015, **21**, 12996; (*b*) M. Tamada, T. Iino, Y. Wang, M. Ide, A. Saeki, H. Furuta, N. Kobayashi and S. Shimizu, *Tetrahedron Lett.*, 2017, **58**, 3151; (*c*) M. Fukuda, S. Mori, H. Furuta and S. Shimizu, *Chem. –Asian. J.*, 2019, **14**, 1697.
14 (*a*) S. Shimizu, *Chem. Commun.*, 2019, **55**, 8722; (*b*) S. Shimizu, T. Iino, A. Saeki, S. Seki and N. Kobayashi, *Chem. – Eur. J.*, 2015, **21**, 2893; (*c*) S. Shimizu, T. Iino, Y. Araki and N. Kobayashi, *Chem. Commun.*, 2013, **49**, 1621.
15 L. Li, L. Wang, H. Tang and D. Cao, *Chem. Commun.*, 2017, **53**, 8352.
16 Y. Zhou, C. Ma, N. Gao, Q. Wang, P.-C. Lo, K. S. Wong, Q.-H. Xu, T. Kinoshita and D. K. P. Ng, *J. Mater. Chem. B*, 2018, **6**, 5570.
17 K. Miki, A. Enomoto, T. Inoue, T. Nabeshima, S. Saino, S. Shimizu, H. Matsuoka and K. Ohe, *Biomacromolecules*, 2017, **18**, 249.
18 C. Wu, X. Huang, Y. Tang, W. Xiao, L. Sun, J. Shao and X. Dong, *Chem. Commun.*, 2019, **55**, 790.
19 R. Ishimatsu, H. Shintaku, Y. Kage, M. Kamioka, S. Shimizu, K. Nakano, H. Furuta and T. Imato, *J. Am. Chem. Soc.*, 2019, **141**, 11791.
20 Y. Kage, S. Mori, M. Ide, A. Saeki, H. Furuta and S. Shimizu, *Mater. Chem. Front.*, 2018, **2**, 112.
21 A. Pickett, A. Mohapatra, A. Laudari, S. Khanra, T. Ram, S. Patil and S. Guha, *Org. Electron.*, 2017, **45**, 115.
22 Y. Yu, Y. Wu, A. Zhang, C. Li, Z. Tang, W. Ma, Y. Wu and W. Li, *ACS Appl. Mater. Interf.*, 2016, **8**, 30328.
23 J. Yu, B. Zhao, X. Nie, B. Zhou, Y. Li and J. Hai, *New J. Chem.*, 2015, **39**, 2248.
24 U. Koldemir, J. S. Tinkham, R. Johnson, B. Lim, H. A. Yemam, K. J. Gagnon, S. Parkin and A. Sellinger, *J. Mater. Chem. C*, 2017, **5**, 8723.
25 A. Rana, Y. Hong, T. Y. Gopalakrishna, H. Phan, T. S. Herng, P. Yadav, J. Ding, D. Kim and J. Wu, *Angew. Chem., Int. Ed.*, 2018, **57**, 12534.
26 (*a*) M. U. Winters, J. Kärnbratt, M. Eng, C. J. Wilson, H. L. Anderson and B. Albinsson, *J. Phys. Chem. C,* 2007, **111**, 7192; (*b*) M. K. Kuimova, M. Balaz, H. L. Anderson and P. R. Ogilby, *J. Am. Chem. Soc.,* 2009, **131**, 7948; (*c*) M. K. Kuimova, S. W. Botchway, A. W. Parker, M. Balaz, H. A. Collins, H. L. Anderson, K. Suhling and P. R. Ogilby, *Nat. Chem.,* 2009, **1**, 69.
27 K. H. Park, S. Ooi, T. Kim, T. Tanaka, A. Osuka and D. Kim, *Phys. Chem. Chem. Phys.* 2016, **18**, 23374.
28 C.-Z. Li, H.-L. Yip and A. K.-Y. Jen, *J. Mat. Chem.,* 2012, **22**, 4161.
29 T. M. Clarke and J. R. Durrant, *Chem. Rev.*, 2010, **110**, 6736.
30 M. C. Scharber, D. Mühlbacher, M. Koppe, P. Denk, C. Waldauf, A. J. Heeger and C. J. Brabec, *Adv. Mater.*, 2006, **18**, 789.
31 B. P. Rand, D. P. Burk and S. R. Forrest, *Phys. Rev. B*, 2007, **75**, 115327.